Fulfillment of expectations of precise measurements of the Casimir force

V.B. Svetovoy* and M.V. Lokhanin
Department of Physics, Yaroslavl State University,
Sovetskaya 14, Yaroslavl 150000, Russia
(February 1, 2008)

We compare theoretical expectations for the Casimir force with the results of precise measurements. The force is calculated at finite temperature for multilayered covering of the bodies using the Lifshitz theory. We argue that the dielectric function of the metallization has to be directly measured to reach the necessary precision in the force calculation. Without knowledge of this function one can establish a well defined upper limit on the force using parameters of perfect single-crystal materials. The force measured in the torsion pendulum experiment does not contradict to the upper limit. Importance of a thin Au/Pd layer in the atomic force microscope experiments is stressed. The force measured with the microscope is larger than the upper limit at small separations between bodies. The discrepancy is significant and reproduced for both performed measurements. The origin of the discrepancy is discussed. The simplest modification of the experiment is proposed allowing to make its results more reliable and answer the question if the discrepancy has any relation with the existence of a new force.

12.20.Ds, 03.70.+k

I. INTRODUCTION

The Casimir force [1] (see [2] for a review) between closely spaced macroscopic bodies is an effect of quantum electrodynamics (QED) and for this reason it could be predicted very accurately. The force acting between nonideal bodies can be found using the Lifshitz theory [3,4], where it depends on optical properties of used materials. Knowledge of these properties is the weakest element in the theory restricting the accuracy that can be achieved. Experiments measuring the Casimir force are of great importance because they are sensitive to the presence of new fundamental forces [5,6] predicted in many modern theories (see [7,8] and references therein). To distinguish a new force from the background, we should be able to calculate the Casimir force with a precision better than the experimental one. In the series of recent experiments this force has been measured with the torsion pendulum (TP) [9] in the range of distances $0.6-6\ \mu m$ and with the atomic force microscope (AFM) [10–12] in the range $0.1-0.9\ \mu m$. The corresponding precisions were 5% and 1%, respectively.

For two ideal plates the famous Casimir formula [1] for the force per unit area is

$$F_c^{pl}(a)=\frac{\pi^2\hbar c}{240a^4}, \tag{1}$$

where a is the distance between plates. In the experiments the force is measured between metallized disc and sphere because for two plates it is difficult to keep them parallel. In this case (1) has to be modified with the proximity force theorem (PFT) [13]. This theorem allows to evaluate the force by adding the contributions of various distances as if they were independent and for plate and sphere it is reduced to

$$F(a)=2\pi R\int_a^{R+a}F^{pl}(x)\,dx, \tag{2}$$

where R is the radius of curvature of the spherical surface. The PFT approximation is good for $R\gg a$ that holds true in all the experiments. If we use the Casimir expression (1) for the force in (2), then the force between plate and sphere will be

$$F_c^0(a)=\frac{\pi^3\hbar c}{360}\frac{R}{a^3}. \tag{3}$$

*E-mail: svetovoy@nordnet.ru

Eq. (3) was deduced for ideally conducting bodies at zero temperature and three kinds of corrections have been considered to take into account their real properties. The correction due to finite metal conductivity was found [14,15] on the base of the free electron model, where the optical properties of a metal were described by the only parameter ω_p which is the plasma frequency. The force including corrections up to the second order [16] is

$$F_c^p(a) = F_c^0(a)\left[1 - 4\frac{c}{a\omega_p} + \frac{72}{5}\left(\frac{c}{a\omega_p}\right)^2\right]. \tag{4}$$

For typical plasma frequency $\omega_p \sim 10^{16}\ s^{-1}$ and separations $a \leq 1\ \mu m$ the correction will be more than 10%. Correction due to finite temperature has been found [17] for ideal conductors and the resulting force is given by

$$F_c^T(a) = F_c^0(a)\left(1 + \frac{720}{\pi^2} f(\xi)\right), \tag{5}$$

where $\xi = k_B T a/\hbar c \approx a(\mu m)/7.61$ for $T = 300^\circ K$. The function $f(\xi)$ is expressed via an infinite sum but it can be represented approximately as $f(\xi) = (\xi^3/2\pi)\zeta(3) - (\xi^4\pi^2/45)$ for $\xi < 1/2$. The temperature correction is negligible for the AFM experiments [10,12] since ξ is small in the important separation range $0.1 - 0.3\ \mu m$ and is only a minor correction in condition of the TP experiment [9], where the important separation range was $0.6 - 3\ \mu m$. The general form of the correction due to surface distortions has been found in [18]. If the bodies are covered by distortions with characteristic amplitudes A_1 and A_2, then the force up to the second order in the relative amplitudes of the distortions has the form

$$F_c^d(a) = F_c^0(a)\left[1 + 3\left(\langle f_1\rangle\frac{A_1}{a} - \langle f_2\rangle\frac{A_2}{a}\right) + 6\left(\left\langle f_1^2\right\rangle\frac{A_1^2}{a^2} - 2\langle f_1 f_2\rangle\frac{A_1 A_2}{a^2} + \left\langle f_2^2\right\rangle\frac{A_2^2}{a^2}\right)\right], \tag{6}$$

where the functions $f_{1,2}(x,y)$ describe distribution of the distortions on the surfaces and $\langle ...\rangle$ denotes averaging over the surface area. Corrections due to surface roughness are very important for the experiment [10].

At first [9–11,19] the experimental data were treated using these corrections to Eq. (3), but it was realized soon that at least the conductivity correction has to be considered on more reliable basis. In more realistic approach the Lifshitz theory [4] was used to evaluate the force between bodies [12,20]. Similar but technically a little bit different method was developed in [21]. In these approaches the force depends on the dielectric function of the bodies at imaginary frequencies $\varepsilon(i\omega)$. It has to be expressed with the dispersion relation via the imaginary part of the function $\varepsilon(\omega)$ on the real axis which can be directly measured. However, in any of the experiments the information on $\varepsilon(\omega)$ was not collected and the handbook data were used instead. Such data are good only to make an estimate for the Casimir force with the accuracy much worse than the experimental one. The reason is that the dielectric function depends in substantial degree on the sample preparation procedure as will be discussed below. Nevertheless, it is possible to find [23] a reliable upper limit on the Casimir force using only well defined parameters of perfect crystalline materials. In this paper we will discuss in detail this limit and its comparison with the existing experimental data.

The paper is organized as follows. In Sec. II we give a general expression for the Casimir force between sphere and plate made of nonideal materials at nonzero temperature. Then, to treat the experimental data, the expression for the force is generalized for the case of layered bodies. The choice of dielectric functions and parameters for the used materials is described in Sec. III. In Sec. IV we define the boundary values of the optical parameters and find the upper limit on the force in conditions of each independent experiment. Possible reasons for discrepancy between theory and experiment are discussed in Sec. V. Our conclusions are given in the last Section.

II. THEORY

Let us discuss first a reliable way to evaluate the Casimir force in the experimental configurations. The force per unit area between parallel plates arising as a result of electromagnetic fluctuations is generalized by the Lifshitz theory [4], where the real material is taken into account by its dielectric function at imaginary frequencies $\varepsilon(i\zeta)$:

$$F^{pl}(a) = \frac{kT}{\pi c^3}{\sum_{n=0}^{\infty}}' \zeta_n^3 \int_1^\infty dp p^2 \left\{\left[G_1^2 e^{2p\zeta_n a/c} - 1\right]^{-1} + \left[G_2^2 e^{2p\zeta_n a/c} - 1\right]^{-1}\right\}. \tag{7}$$

Here prime over the sum sign means that $n=0$ term is taken with the coefficient $1/2$ and

$$G_1=\frac{p+s}{p-s},\quad G_2=\frac{\varepsilon\left(i\zeta_n\right)p+s}{\varepsilon\left(i\zeta_n\right)p-s},$$

$$s=\sqrt{\varepsilon\left(i\zeta_n\right)-1+p^2},\quad \zeta_n=\frac{2\pi nkT}{\hbar}. \tag{8}$$

It is supposed that both bodies were made of identical materials. The function $\varepsilon\left(i\zeta_n\right)$ cannot be measured directly but can be expressed via imaginary part of the dielectric function $\varepsilon''\left(\omega\right)$ on the real axis with the dispersion relation

$$\varepsilon\left(i\zeta\right)-1=\frac{2}{\pi}\int\limits_0^\infty d\omega\frac{\omega\varepsilon''\left(\omega\right)}{\omega^2+\zeta^2}. \tag{9}$$

Information on $\varepsilon''\left(\omega\right)$ can be extracted from the data on reflectivity and absorptivity of electromagnetic waves with the frequency ω for a given material.

Applying PFT to Eq. (7) one can find the force between sphere and plate. The integration in (2) can be done analytically and we find

$$F(a)=-\frac{kTR}{c^2}{\sum_{n=0}^{\infty}}'\zeta_n^2\int\limits_1^\infty dpp\ln\left[\left(G_1^{-2}e^{-2p\zeta_n a/c}-1\right)\left(G_2^{-2}e^{-2p\zeta_n a/c}-1\right)\right]. \tag{10}$$

Special care needs to treat the first $n=0$ term. The formal reason is that ζ_n^2 becomes zero but the integral over p diverges. The physical reason is that this term corresponds to the static limit when for metallic bodies $\varepsilon\to\infty$. This means that any parameter characterizing the dielectric function of a metal cannot appear in the $n=0$ term in contrast with a dielectric for which it will depend on the static permittivity of the material. In the $\varepsilon\to\infty$ limit the functions $G_{1,2}$ become $-G_1=G_2=1$. The formal problem is overcome by introducing the integration over a new variable $x=2p\zeta_n a/c$ and after that one can take $\zeta_n=0$ for the $n=0$ term. The resulting contribution of the first term in the force corresponds to the classical limit $F_{cl}\left(a\right)$ for metals

$$F_{cl}\left(a\right)=\frac{kTR}{4a^2}\zeta\left(3\right), \tag{11}$$

where $\zeta\left(n\right)$ is the zeta-function. Note that in this limit the force does not depend on the metal parameters as it should be for a static field.

The bare Casimir force (3) is reproduced from Eq. (10) in the limit $\varepsilon\to\infty$ and $T\to 0$. The finite conductivity correction also can be derived from (10). To this end one considers the limit of small temperature when the sum in (10) can be replaced by the integral and supposes that the dielectric function of the metal covering the bodies is described by the free electron plasma model. In this model $\varepsilon\left(i\zeta\right)$ is

$$\varepsilon\left(i\zeta\right)=1+\frac{\omega_p^2}{\zeta^2}, \tag{12}$$

where ω_p is the free electron plasma frequency. Typical value of the frequency $\omega_p\sim 10^{16}\ s^{-1}$ is larger than fluctuation frequencies $\zeta\sim c/a$ giving the main contribution in (10). Then one can expand the functions $G_{1,2}$ in (10) in powers of the parameter ζ/ω_p and performing necessary integrations one finds exactly the result (4) for the conductivity corrections [1]. In this way the corrections up to the fourth order were found in recent paper [24]. The temperature correction (5) is also reproduced from (10) in the limit of ideal metals $\varepsilon\to\infty$. In this case the linear in temperature correction does not survive since the $n=0$ term (11) is exactly canceled by the linear in T contribution from the rest terms in the sum. As a result the leading correction behaves only as ξ^3.

The expression (10) differs from those used in [12] and [20] in two respects. First, in the cited papers the integration connected with the PFT was not done analytically that complicated numerical analysis. Second, the zero temperature

[1]The correction is actually connected with finite density of free electrons (finite ω_p) since the metal conductivity is still infinite for the plasma model. Nevertheless, we will not change the fixed terminology.

limit has been taken. This limit was also considered in [21], though the PFT integral was evaluated explicitly. It seems a reasonable approximation at small separations because the temperature correction in (5) is proportional to ξ^3 and, therefore, is small. However, one should remember that this correction was derived in the limit of ideal conductors $\varepsilon \to \infty$. For a real conductor it will be proportional to ξ as expected for difference between sum and integral and will be important (for details see [25]). We have computed the force according to (10) and with the integral instead of the sum at the smallest separation $a = 100\ nm$ tested in the experiments. For the plasma model (12) with $\omega_p = 2 \cdot 10^{16}\ s^{-1}$ we have found that the difference between the sum and integral is 2.5 pN for $T = 300^\circ\ K$. It becomes 4 pN for the Drude dielectric function (see Eq. (18) below) with the damping frequency $\omega_\tau = 5 \cdot 10^{13}\ s^{-1}$. These values exceed the conservative estimate for the experimental errors 2 pN [12].

In the AFM experiments an additional $Au_{0.6}Pd_{0.4}$ layer of 20 nm [10] or 8 nm [11,12] thick was on the top of Al metallization of the bodies to prevent aluminum oxidation. It has to be included into consideration. This layer is transparent for the electromagnetic waves with high frequencies $\sim c/a$ since adsorption, proportional to $\varepsilon''(\omega)$, is small. For this reason the layer was ignored in [10–12]. However, the force depends on $\varepsilon(i\zeta)$ for which the low frequencies dominate in the dispersion relation (9) because of large $\varepsilon''(\omega)$ and that is why we cannot neglect the Au/Pd layer. To take it into account, one has to generalize expression for the force (7) to the case of layered bodies. Suppose that the top layer has the thickness h and its dielectric function is ε_1. The bottom layer is thick enough to be considered as infinite and let its dielectric function be ε_2. The method described in [4] for deriving Eq. (7) can be easily generalized for layered plates. We have to add only the matching conditions for the Green functions on the layers interface. After some algebra the result will look exactly as (7) but with more complex $G_{1,2}$:

$$G_1 = \frac{(s_1+s_2)(p+s_1)e^{\zeta_n s_1 h/c} + (s_1-s_2)(p-s_1)e^{-\zeta_n s_1 h/c}}{(s_1+s_2)(p-s_1)e^{\zeta_n s_1 h/c} + (s_1-s_2)(p+s_1)e^{-\zeta_n s_1 h/c}},$$

$$G_2 = -\frac{(\varepsilon_2 s_1+\varepsilon_1 s_2)(\varepsilon_1 p+s_1)e^{\zeta_n s_1 h/c} + (\varepsilon_2 s_1-\varepsilon_1 s_2)(\varepsilon_1 p-s_1)e^{-\zeta_n s_1 h/c}}{(\varepsilon_2 s_1+\varepsilon_1 s_2)(\varepsilon_1 p-s_1)e^{\zeta_n s_1 h/c} + (\varepsilon_2 s_1-\varepsilon_1 s_2)(\varepsilon_1 p+s_1)e^{-\zeta_n s_1 h/c}}, \tag{13}$$

where $s_{1,2}$ are defined similar to s in (8). The force between plate and sphere is given by (10) with the above $G_{1,2}$.

To see qualitatively the effect of an additional layer, we found the finite conductivity correction up to the second order in this case. Than for the force one has

$$F_c^p(a,h) = F_c^0(a)\left[1 - 4K(h)\frac{c}{a\omega_{1p}} + \frac{72}{5}\left(K(h)\frac{c}{a\omega_{1p}}\right)^2\right], \tag{14}$$

where the function $K(h)$ depends on the plasma frequencies of the layers ω_{1p} , ω_{2p} and the thickness of the top layer h

$$K(h) = \frac{\omega_{1p} + \omega_{2p}\tanh(h\omega_{1p}/c)}{\omega_{2p} + \omega_{1p}\tanh(h\omega_{1p}/c)}. \tag{15}$$

When $h = 0$ the force will depend only on ω_{2p} and in the case $h \to \infty$ on ω_{1p} as it should be. The effect of the top layer disappears if the plasma frequencies coincide. The top layer will be negligible if $h\omega_{1p}/c \ll 1$. For typical plasma frequencies $\sim 10^{16}\ s^{-1}$ it is definitely not the case even for $h = 8\ nm$. The opposite conclusion made in [19] was based on the too small value of ω_p for gold as will be discussed below (see also [21]). Eq. (14) is not very good approximation and was discussed only for qualitative understanding of the effect. For actual calculations we will use the exact equations (10), (13).

Importance of a thin metallic layer on the body surfaces has been stressed first in [26]. The general expression for the Casimir force between layered bodies has been presented in [21] but was not used their for actual calculations. Significant role of the Au/Pd layer in the AFM experiments was indicated in our preprint [23], where it was demonstrated that the effect far exceeds the experimental errors. This conclusion was supported in [27], where the expressions (13) for $G_{1,2}$ were confirmed using a different method to deduce them. However, the authors were uncertain on applicability of (13) for thin films with $h < 25\ nm$ because the spatial dispersion of the dielectric function can be important for such films. We discuss this effect in Sec. V where we argue that the spatial dispersion can be neglected because of very short mean free path for the electrons in thin films.

III. THE DIELECTRIC FUNCTION

Now we are able to evaluate the Casimir force in real geometry of the experiments if there is information on the dielectric functions of used materials: Au, Al, and $Au_{0.6}Pd_{0.4}$ alloy. Strictly speaking, one has to measure these

functions in wide range of wavelengths on the same samples which are used for the force measurement. It was not done in all of the experiments and to draw any conclusion from them we have to make some assumptions on the dielectric functions. At low frequencies Au and Al are well described by the Drude dielectric function [28]:

$$\varepsilon = \varepsilon' + i\,\varepsilon'',$$

$$\varepsilon'(\omega) = 1 - \frac{\omega_p^2}{\omega^2 + \omega_\tau^2}, \qquad \varepsilon''(\omega) = \frac{\omega_p^2 \omega_\tau}{\omega\left(\omega^2 + \omega_\tau^2\right)}, \tag{16}$$

where ω_p is the free electron plasma frequency and ω_τ is the Drude damping frequency. A simple test for validity of the Drude model is behavior of the material resistivity [29] which is defined as

$$\rho(\omega) = Im\left(\frac{1}{\varepsilon_0\left(1 - \varepsilon(\omega)\right)\omega}\right) = \frac{\omega_\tau}{\varepsilon_0 \omega_p^2}, \tag{17}$$

where ε_0 is the free space permittivity. The resistivity is frequency independent within the Drude approximation. For high-purity single-crystal samples of Au and Al (entries 2 in Table I) the frequency behavior of the resistivity in the infrared range of wavelengths $3\ \mu m < \lambda < 32\ \mu m$ is shown in Fig. 1. The data on the dielectric functions were taken from [30], where the results from many original works are collected. The data for $\varepsilon'(\omega)$ and $\varepsilon''(\omega)$ can be fitted with (16) to find the parameters ω_p and ω_τ. The points and fitting curves for $\varepsilon''(\omega)$ are shown in the same Fig. 1. Palladium definitely cannot be described by (16) since its resistance significantly changes in the infrared range. However, it is known experimentally that amorphous metallic alloys can be described by the Drude approximation [29]. The physical explanation for this is associated with large Drude damping of the compounds like $Au_{0.6}Pd_{0.4}$.

Of course, at higher frequencies when interband transitions are reached the Drude approximation fails. Nevertheless, it is very helpful since low frequencies dominate in the dispersion relation. Extrapolating (16) to all frequencies one finds

$$\varepsilon(i\zeta) = 1 + \frac{\omega_p^2}{\zeta\left(\zeta + \omega_\tau\right)}. \tag{18}$$

Let us estimate the relative error inserted in (18) due to extrapolation. If ω_0 is the frequency of the first resonance for a given metal, then the contribution in $\varepsilon(i\zeta)$ of the frequency range $\omega_0 < \omega < \infty$, where the Drude model does not valid, will be $\left(\omega_p/\zeta\right)^2 \cdot \left(\omega_\tau/\omega_0\right)$ for $\zeta \geq \omega_0$. This contribution one can take as an estimate for the absolute error and, therefore, for the relative error one has $\sim \omega_\tau/\omega_0$. For typical values $\omega_\tau \sim 10^{14}\ s^{-1}$ and $\omega_0 > 10^{15}\ s^{-1}$ the error can be as large as 10% but error in the force is smaller. If we will use (18) for the force computation and change ω_p by 5% (10% correction to $\varepsilon(i\zeta)$ at all frequencies) then the force is changed less than 2%. Moreover, since the interband transitions give a correction to (18) which is frequency dependent, it reduces the correction to the force further. Of course, we can take the interband transitions into consideration exactly using the handbook data in visible-ultraviolet range which are not very sensitive to the purity and defect density as it happens in the infrared range. However, we are intended to establish the upper limit on the force using ω_p in (18) which is definitely larger than any real value and for this reason we can neglect the interband transitions.

Therefore, in all cases of interest we can use Eq. (18) to describe the dielectric function of a material on the imaginary axis. The question is how we should extract the parameters ω_p and ω_τ from the data. We proceeded as follows. The data for the complex refraction index $n + i\kappa = \sqrt{\varepsilon}$ have been taken from [30]. First, the validity of the Drude approximation was checked by calculating the frequency dependence of the material resistivity according to (17). In the investigated cases the resistivity is more or less constant in the wavelength range $\lambda > 2\ \mu m$ ($\omega < 9.4 \cdot 10^{14}\ s^{-1}$). This range gives the most important contribution to the dispersion relation (9) and, therefore, it is the range where we have to extract the Drude parameters. Using ω_p found from the high frequency region can happen to be wrong. For example, sometime the plasma frequency is estimated using the transition point in the reflectivity dependence on frequency. It works, not very good though, for Al but gives considerably smaller value for Au than that found from fitting $\varepsilon(\omega)$ in the infrared range. Probably such an estimate was taken in [9,19] for Au where very small value $\omega_p = 3.6 \cdot 10^{15}\ s^{-1}$ was used.

The optimal fitting procedure is described in [28]. The damping frequency is evaluated first from the ratio $\left(1 - \varepsilon'\right)/\varepsilon''$ which depends linearly on frequency in the Drude model

$$\frac{1 - \varepsilon'}{\varepsilon''} = \frac{\omega}{\omega_\tau}. \tag{19}$$

After that ω_p^2 can be extracted from $1 - \varepsilon'$ by linear fit. The results together with the statistical errors are collected in Table I for those data in [30] which include the optical behavior of Au and Al in the infrared region. This table clearly

demonstrates that the Drude parameters depend significantly on the sample which is used to measure the optical data. These samples contained different densities of the defects (such as impurity atoms, vacancies, dislocations, etc.) that influence their optical properties. In this sense there are no universal material parameters. Reproducible parameters one can get only for high-purity single-crystals. In this connection all the attempts to use the handbook data for the Casimir force calculation can be considered only as estimates and cannot claim on high precision.

Actually in any of the experiment we do not know the Drude parameters even with 10% accuracy. That is because the optical properties of evaporated or spattered films which cover the bodies can be quite different from those of bulk materials and depend on technological details of film preparation. It is known, for example, that the film density is typically 0.7 from that of the bulk material if it was not annealed. For the resistivity of spattered and evaporated Au [32] the value $\rho_0 = 8.2\ \mu\Omega \cdot cm$ has been reported in contrast with the bulk resistivity $2.25\ \mu\Omega \cdot cm$. If a metal is evaporated or spattered on a substrate, it has a large number of defects. Relatively thick metallic films ($> 100\ nm$) are usually exist in polycrystalline form. Defects will reduce the concentration of free electrons n which defines the plasma frequency of the material. They also will increase the damping frequency ω_τ and resistivity since the mean free path of electrons will shorten. To minimize these undesirable in practical applications effects the films are usually annealed at high temperature. In the experiments [9–12] it was not reported were the bodies annealed or not but one can say definitely that it was not done in the AFM experiments because the polysterene ball cannot exist at the annealing temperature. Even more defects present in thin films ($\leq 20 - 30\ nm$) which are usually amorphous. This explains why thin films have very large resistivity in comparison with the bulk material. Entries 1 and 4 for Al in Table I correspond to the data for thick film samples. They support our expectations that the plasma frequency for films should be smaller and the resistivity larger than those for the bulk material.

IV. THE UPPER LIMIT

Though we cannot use the handbook data to evaluate the force, one can constrain it for a given experiment. This statement is based on the observation that the force (10) increases every time when ω_p increases or ω_τ decreases. It has simple physical meaning: the force becomes larger when the metal reflectivity increases. For us it is important that any technological procedures will reduce ω_p and increase ω_τ for a given material. A perfect single-crystal will have the largest plasma frequency and the smallest ω_τ and these parameters are well defined. One can use them to get the upper limit on the Casimir force. The plasma frequency ω_p is defined by the concentration of free electrons in the metal n and their effective mass m_e^*

$$\omega_p = \sqrt{\frac{e^2 n}{m_e^* \varepsilon_0}}, \tag{20}$$

where e is the electron charge. For good metals, which we are concerned, m_e^* is close but larger than the electron mass. It will be helpful for what follows to use Eq. (17) and instead of the damping frequency ω_τ take the static resistivity $\rho(0) = \rho_0$ as a parameter. The later can be directly measured for any material.

A. Torsion pendulum experiment

In the TP experiment [9] the quartz lens and plate were covered first with Cu of thickness $0.5\ \mu m$ and then with Au of the same thickness. The Au layer is thick enough to be considered as infinite and Cu will not play any role. We will find the upper limit on the electron concentration if suppose that every Au atom produce a free electron with the mass $m_e^* = m_e$. Then for the Au plasma frequency one finds $\omega_p^{Au} = 1.37 \cdot 10^{16}\ s^{-1}$. The resistivity for crystalline gold is $\rho_0^{Au} = 2.25\ \mu\Omega \cdot cm$. One can compare these parameters with that given in Table I to make sure that they correspond to the limit values. Substituting these parameters in (18) and calculating the force according to (10) one finds the upper limit on the Casimir force $F^{max}(a)$ in the TP experiment.

To compare the upper limit on the force with the measured force F^{exp}, it is more convenient to consider the residual force defined as[1]

$$\Delta F(a_i) = F^{exp}(a_i) - F^{max}(a_i), \tag{21}$$

[1]Note that Lamoreaux [9] used different definition of the residual force $F^{exp}(a_i) - F_c^0(a_i)$.

where a_i are the separations for which the force has been measured. Theory and experiment will be in agreement if ΔF will not be positive within the experimental errors. The original experimental data were presented for the lens curvature radius $R = 11.3\ cm$ and the residual force in this case is shown in Fig. 2a. It clearly indicates the presence of some unexplained force at the smallest separations. However, later the author recognized [26] that he was working with aspheric lens which had the curvature radius $R = 12.5 \pm 0.3\ cm$ in the place where the force was measured. The correction was published in erratum [9]. The points for $\Delta F(a_i)$ with the corrected R are presented in Fig. 2b. This time the prediction obviously does not contradict to the experiment but dealing with the upper limit we cannot conclude that there is an agreement, either.

The question about surface distortions in TP experiment has been raised in [33]. Surfaces of the bodies have not been examined in [9] but roughness of the order of $30-40\ nm$ is quite typical for a metallic film on a polished substrate and correlates with the substrate roughness. Quartz optics is used for near UV light and its surface has to be polished with a precision at least $\lambda/10$, where $\lambda \sim 300\ nm$ is the UV wavelength. It supports the value above which is routinely observed with atomic force or tunnel microscope. According to (6) the short-scale stochastic distortions give only a few percent correction even for the smallest separation $a = 0.6\ \mu m$. Large-scale deviations seem potentially more dangerous [33] since the correction can be the first order in A/a especially if we take into account that the lens was not spherical. The radius r_{int} of the interaction area one can estimate as $r_{int} \sim \sqrt{Ra} \sim 1000\ \mu m$. Therefore, only small area on the lens takes part in the interaction. In this place the lens can be represented as part of the parabolic surface

$$z = \frac{r^2}{2\,(R + \Delta R)} \approx \frac{r^2}{2R} - \frac{1}{2}\frac{r^2}{R^2}\Delta R, \tag{22}$$

where ΔR is the error in the curvature radius. Here the second term describes the error in the plate-lens separation and it can be taken as the distortion amplitude. This amplitude is maximal for $r = r_{int}$ and for the relative amplitude one has an estimate

$$\frac{A}{a} \sim \frac{1}{2}\frac{\Delta R}{R} \simeq 1.2 \cdot 10^{-2}. \tag{23}$$

This value is rather small and according to (6) the correction to the force will be less but comparable with the experimental errors. Moreover, negligible role of the large-scale distortions is actually an experimental fact. The region of the plate and sphere used for the force measurement in [9] was varied by tilting the lens with the adjustment screws and there was no evidence for any variation of the force depending on the region used for the measurement.

The first attempt to evaluate the Casimir force was undertaken by the author of TP experiment [9] who takes into account the first finite conductivity correction but used very small ω_p for Au. Lamoreaux was the first who recognized the necessity of more rigorous approach to the force evaluation [20] and importance of thin films on the metallic surfaces [26]. His numerical results were not quite good due to the delicate problem with choice of ω_p which we discussed above. The matter has been settled in [21,22] with the result which coincide with ours. However, our statement is that the calculated force represents the upper limit but not the force itself. The reason is that evaporated Au film will have smaller plasma frequency than $1.37 \cdot 10^{16}\ s^{-1}$ due to large number of defects in the film. To know the exact value of the force, one has to measure the dielectric function of the bodies but not to take it from a handbook.

B. AFM experiment

Let us discuss now the upper limit on the Casimir force for the AFM experiment [10]. The plasma frequency for Al can be restricted using (20) if one supposes that every atom produces 3 free electrons. It gives $\omega_p^{Al} = 2.40 \cdot 10^{16}\ s^{-1}$ that coincide with the largest value in Table I. The resistivity of perfect crystals is $\rho_0^{Al} = 2.65\ \mu\Omega \cdot cm$. Since we successfully predicted the plasma frequencies for the best samples of Au and Al, the same way one can use to estimate ω_p for Au/Pd. If each Au atom gives one and Pd atom gives not more than two free electrons, then $\omega_p^{Au/Pd} = 1.69 \cdot 10^{16}\ s^{-1}$. This alloy is used in microelectronics and resistivity of the bulk material is known to be $\rho_0^{Au/Pd} \approx 30\ \mu\Omega \cdot cm$ [34] in accordance with the statement that alloys have large Drude damping. These data allow to find the upper limit on the force using (10) with the functions $G_{1,2}$ defined in (13).

Before comparing the upper limit with the measured force we have to discuss a few additional aspects concerning the experiment. Real surface of the bodies is always distorted and the distortions are especially important to treat the data in [10]. The distortion statistics were analysed with the atomic force microscope [19]. The force has to be averaged over the distorted surfaces and we use for this the procedure developed in [19]. The major distortions are the large separate crystals situated irregularly on the surfaces with a typical lateral size of 200 nm. The height of the

highest and intermediate distortions is about $h_1 = 40\ nm$ and $h_2 = 20\ nm$, respectively. The homogeneous stochastic background of the averaged height $h_0/2 = 5\ nm$ fills the surface between the major distortions. The character of roughness on the plate and on the ball is quite similar. The part of the surface occupied by distortions with the height h_1, h_2, and $h_0/2$ was measured as $v_1 = 0.11$, $v_2 = 0.25$, and $v_0 = 0.64$, respectively. These values are the probabilities for the corresponding distortion to appear. The body surface is defined in such a way that averaging over distortions gives zero result. Then the averaged force is the sum of local forces for all possible kinds of distortions which face each other taken with the corresponding probabilities

$$F^{dist}(a) = \sum_{i,j=0}^{2} v_i v_j F(a_{ij}), \tag{24}$$

where a_{ij} are the local separations defined in [19]. For us it will be important that the minimal local separation is $a_{11} = a - 54.8\ nm$. This procedure seems quite reliable but, of course, large distortions give the feeling of uncertainty. The upper limit on the Casimir force has to be averaged with the corresponding roughness parameters according to (24).

The raw force F_m measured in the experiments consists of a few components [10]

$$F_m = F_c(a_1 + a_0) + F_e(a_1 + a_0) + C \cdot (a_1 + a_0). \tag{25}$$

Here a_1 is the separation from the voltage applied to the piezo corrected to the cantilever deflection, a_0 is the parameter chosen in such a way that $a = a_1 + a_0$ is the absolute separation between bodies, the first term in (25) is the Casimir force, the second term is the electrostatic force corresponding to the measured contact potential 29 mV, the third term represents the linearly increasing coupling of the scattered light into the photodiodes (see [10] for details). The parameters a_0 and C were determined at large separations, where F_c is represented by the bare force (3). Then the Casimir force can be extracted from the raw data with the help of (25). Similar way to find the Casimir force was used in [9]. Of course, the separation a has to be defined as the distance between averaged surfaces of Au/Pd layers. However, the role of these layers have been underestimated in [10,19]. In [10] the Casimir force was found from (25) but a was interpreted as the absolute separation between Al surfaces [10,19]. Effectively the Au/Pd layers were changed by Al which has larger ω_p and, therefore, the force calculated theoretically was overestimated.

It was indicated [10] that the thickness of Au/Pd layer is less than 20 nm, that is why for calculations we use the conservative value $h = 15\ nm$. This change makes the force only larger. The experimental points from [10] (triangles) and theoretical upper limit on the force including the roughness correction (solid line) are shown in Fig. 3 in the small separations range $a < 250\ nm$. If the top layer is changed by Al, it enlarges the force on 15 pN at the smallest separation $a = 120\ nm$. It is clear that the top layer definitely cannot be ignored in the force evaluation. Variation of ω_p^{Al} on 10% gives only 1 pN change in the force because of screening effect of the top layer. The same variation in $\omega_p^{Au/Pd}$ changes the force on 2 pN. The resistivity variation of the Au/Pd layer on 30% gives 1 pN effect. At larger separations all the effects become smaller.

We can see from Fig. 3 that the upper limit is smaller than the force measured at small separations and the difference is significant. This conclusion contradicts to that in [19], where good agreement between theory and experiment has been reported (dotted line) based on the detailed theoretical analysis. We have already stressed the importance of the Au/Pd layer but it is not the only reason of deviations. It comes also from poor behavior of the finite conductivity correction used in [19] at small separations a. The correction was based on a simple interpolating formula [16] for the force between two plates

$$F_c^{plates}(a) = F_c^{0\ plates}(a)\left(1 + \frac{11}{3}\frac{c}{a\omega_p}\right)^{-\frac{16}{11}} \tag{26}$$

which is applicable in wider range of separations than the expansion up to the second order (4). It was used to calculate the conductivity correction between sphere and plate. Applying the proximity force theorem to (26) one gets

$$F(a) = 3F_c^0(a)\int_1^\infty \frac{dx}{x^4}\left(1 + \frac{11}{3x}\frac{c}{a\omega_p}\right)^{-\frac{16}{11}}, \tag{27}$$

where the upper limit was moved to infinity since $a \ll R$. This integral can be expressed via the Gauss hypergeometric function but in [19] it was expanded in the series up to the fourth order

$$F(a) = F_c^0(a)\left[1 - 4\frac{c}{a\omega_p} + \frac{72}{5}\left(\frac{c}{a\omega_p}\right)^2 - \frac{152}{3}\left(\frac{c}{a\omega_p}\right)^3 + \frac{532}{3}\left(\frac{c}{a\omega_p}\right)^4\right] \tag{28}$$

and the equations (24) and (28) were used to get the theoretical prediction for the corrected Casimir force (dotted line in Fig. 3). We found that the interpolating curve which we got by numerical intergation of (27) is very close to the exact force evaluated according to (10), (8) with the parameters $\omega_p = 1.88 \cdot 10^{16}\ s^{-1}$, $\omega_\tau = 0$ from [19] and $T = 300°K$ in all range of distances. The small difference between the curves is the temperature effect which disappears when $T \to 0$. However, the expansion (28) works very bad at $a < 100\ nm$. Although the separation in the experiment exceeds 100 nm, the local distance in (24) can be as small as 65 nm, where (28) is absolutely unacceptable. The same is true if one uses the expansion up to the fourth order found in [24] directly form (10). The dashed line in Fig. 3 shows the force calculated according to (24), (27) with the parameters above. The divergence of the solid and dashed curves is the effect of the top layer and different parameters used for Al. The larger ω_p^{Al} which we are using for the upper limit is partly compensated by the top layer and that is why the dashed curve lies not too far from the solid one.

C. Improved AFM experiment

Very important progress has been achieved in [12] where controlled metal evaporation and smaller thickness of Au/Pd layer ($h = 8\ nm$ instead of 20 nm) allowed to reduce the surface roughness to the level when the correction to the force becomes practically unimportant. Also the contact potential has been considerably reduced and the parameter a_0 defining the absolute separation of the surfaces has been found in independent electrostatic measurements. Interaction between metallized ball and corrugated plate has been probed in [11]. It is not a subject of our consideration here. The data for flat plate and sphere in this work are actually in very good agreement with that given in [12] and we will not discuss them specially. The roughness parameters have been reduced to the following [12]: $h_1 = 14\ nm,\ v_1 = 0.05;\ h_2 = 7\ nm,\ v_2 = 0.11;\ h_0/2 = 2\ nm,\ v_0 = 0.84$. Unfortunately, the unjustified assumption that the force is insensitive to the presence of Au/Pd layer has been inserted in the procedure of the Casimir force extraction from the raw data and the following relation has been used instead of (25)

$$F_m = F_c(a + 2h) + F_e\,(a) + Ca. \tag{29}$$

For this reason we cannot directly use the data in [12] to compare with the theoretical prediction. It becomes obvious if we plot in the same figure the measured force in the experiments [10] and [12] (see Fig. 4). One would expect that for thicker Au/Pd layer the force has to be smaller, but the actual relation is opposite and the difference is large. Fortunately, it is easy to restore the right data. In [12] a_0 was found from an independent electrostatic measurement and the constant C was determined at large separations when the shift on $2h = 16\ nm$ in F_c argument was practically unimportant. The measured Casimir force F_{c-m} was expressed as

$$F_{c-m}(a + 2h) = F_m(a) - F_e(a) - Ca, \tag{30}$$

but the points in Fig. 4 taken from [12] represent the force as a function of true separation. Therefore, the force presented in the figure was calculated as

$$F_{c-m}(a) = F_m(a - 2h) - F_e(a - 2h) - C(a - 2h). \tag{31}$$

The Au/Pd layer certainly cannot be ignored and the right expression for the measured Casimir force must be

$$F_{c-m}(a) = F_m(a) - F_e(a) - Ca. \tag{32}$$

It is obvious that to restore the right data one has to shift the open squares in Fig. 4 on $2h = 16\ nm$ to larger separations. After this shift a good agreement between two different experiments is reached. To be absolutely sure that the right transformation was done we have tried to reproduce the measured force directly from the raw data presented in [10] and [12], where the procedure has been described in details. The data were available only for one scan and for this reason our calculations had restricted precision, but it was enough to make a conclusion on reproducibility. To check the procedure, we successfully reproduced the force from the raw data in [10]. The force found from the raw data in [12] according to (32) agrees much better with the shifted points than with the ones presented in [12]. These detailed explanations are given not only to answer the criticism of our preprint [23] but also because of great importance of the conclusion. It is stated in [35,27] that the points have to be shifted to smaller separations. Even

ignoring the arguments above it is obvious from Fig. 4 that such a shift would give drastic disagreement between two experiments made by the same method.

The upper limit on the Casimir force in conditions of the experiment [12] one can find exactly as was explained above. The only difference is the other set of roughness parameters, but in this case the roughness correction is on the level of experimental errors. The experimental points from [12] shifted on 16 nm as was discussed above and the corresponding upper limit (solid line) are presented in Fig. 5. Again we can see that the upper limit is smaller than the measured force and deviation increases at smaller separations. Moreover, even if we replace the 8 nm thick top layer by Al with the maximal plasma frequency $\omega_p = 2.40 \cdot 10^{16}\ s^{-1}$, this disagreement will not disappear as shows the dashed line. The residual force defined according (21) in the experiments [10] (triangles) and [12] (open squares) is shown in Fig. 6. It clearly demonstrates the presence of some unexplained attractive force which is decreasing rapidly when the distance between bodies increased. The points from two different experiments are in reasonable agreement with each other that means that the residual force is reproducible. The residual force becomes larger if we deviate the parameters from their limit values but the agreement between two experiments is not broken.

V. DISCUSSION

Let us discuss now possible reasons for disagreement between experiment and theoretical expectations. As was mentioned above the main problem is the values of the material parameters which can significantly deviate from their handbook values for evaporated or spattered metallic films. The idea of this paper was to find the upper limit on the force instead of the force itself. It allowed to use only well defined parameters of perfect single-crystal materials. We took the largest values for the plasma frequencies and the smallest ones for the resistivities. Any possible deviation from these values will make the force only smaller and disagreement between theory and experiment will be larger.

Some doubts were raised [27] about the possibility to describe the thin top layer by a dielectric function which depends only on frequency. It was stated that the spatial dispersion can be important for thin films because the distance traveled by electron during one period of the field can be larger than the film thickness

$$\frac{v_F}{\omega} > h, \tag{33}$$

where v_F is the velocity of the electron on the Fermi surface. This dimensional effect is really exist (see, for example, [36]) but it is difficult for observation at room temperature. The reason is that for thin metallic films the mean free path for electrons is very short ($< 100\ \mathring{A}$) because of large concentration of the defects. Typically the resistivity of very thing films is on the level of 100 $\mu\Omega \cdot cm$. Then for $\omega_p \sim 10^{16}\ s^{-1}$ from (17) one finds $\omega_\tau \sim 10^{15}\ s^{-1}$. The mean free path is estimated as

$$l = \frac{v_F}{\omega_\tau} \sim 10\ \mathring{A} \tag{34}$$

that is smaller than the used Au/Pd film thickness and, therefore, the spatial dispersion can be neglected. That is why the standard dependence for the dielectric function $\varepsilon(\omega)$ is widely used in optics of metals up to the film thickness in a few nanometers when quantum effects become involved. For the same reason one can neglect the anomalous skin effect for evaporated (spattered) films even for thick ones. Extremely high resistivity 2000 $\mu\Omega \cdot cm$ for 60 nm thick Au/Pd film has been reported in [37]. However, the authors themselves stress that the resistance of the film is, to all appearance, dominated by grain boundaries but optical properties of the film are quite usual. This example shows once more that the details of the spattering technology cannot be ignored.

In [21] uncertainty was expressed about applicability of the proximity force theorem. At the moment there is no any work where the force between sphere and plate was calculated from "the first principles". There are some heuristic approaches [2] allowing to calculate nonadditive Casimir force which agree well with the result found by using PFT (see additional discussion and references in [27]). The PFT states that the main contribution to the force can be found by adding the contributions of various distances as if they were independent and it is applicable to nonadditive forces. An example is the electrostatic force which is nonadditive because the surface charge density is nonuniform for curved surfaces. One can check that the PFT gives in this case the correct result with the accuracy $\sim a/R$. For the discussed experiments the correction is very small ($a/R \sim 0.001$). Even if this term appears with a large coefficient, say ~ 10, the correction will be only on the level of the experimental errors.

In the AFM experiments the electrostatic attraction between bodies because of contact potential was carefully taken into account. Of course, the aluminum surfaces were partly oxidized and electrons could be trapped in the oxide. These charges can be potentially dangerous if the Au/Pd film is not continuous. In this case the trapped charges and their images in underlying aluminum will be the source of the dipole field. Then an additional force can arise as

a result of dipole-dipole interaction. However, it is difficult to make a reliable estimate for this effect because we do not know the concentration of trapped charges and the size of islands in Au/Pd layer or even do discontinuities exist at all for the used layer thickness (it depends on details of the covering procedure). In this connection to make the experiment absolutely clear, it is preferable to use Au instead of Al metallization because its non-reactive surface has strong advantage over Al. It excludes also additional uncertainties connected with Au/Pd layer. One can use as well silver or copper but they are not as inert as gold. It is difficult to measure the dielectric function at the wavelengths larger than 30 μm but this range gives an important contribution to the dispersion relation. That is why the material behavior in this range has to be predictable. One can say definitely that the materials of platinum group cannot be used since they are not described by the Drude dielectric function at low frequencies.

One can speculate that the observed discrepancy is explained by a new Yukawa force mediated by a light scalar boson. Then interaction of two atoms is described by the Yukawa potential

$$V_Y(r) = -\alpha N_1 N_2 \frac{\hbar c}{r} \exp(-r/\lambda), \tag{35}$$

where α is a dimensionless interaction constant, λ is the Compton wavelength of a particle responsible for the interaction, and $N_{1,2}$ is the number of nucleons in atoms of the interacting bodies. An additional advantage of Au metallization is higher density of the bodies coating. In this case the Yukawa force will be enlarged roughly by the factor $(\rho_{Au}/\rho_{Al})^2 \approx 50$, where $\rho_{Au,Al}$ are the material densities. If the observed discrepancy has relation with the Yukawa interaction, the AFM experiment with Au metallization of the bodies will definitely reveal this new force even without detailed knowledge of optical properties of the metallization.

VI. CONCLUSION

We have analysed the results of recent precise measurements of the Casimir force using the Lifshitz theory to evaluate the force. Layered structure of the bodies coating was taken into account in the frame of the Lifshitz approach. It was stressed that the force cannot be predicted with necessary accuracy if there is no detailed information on the dielectric function of the bodies coating. Fortunately, all the used materials (Au, Al and $Au_{0.6}Pd_{0.4}$) are well described in terms of Drude parameters ω_p and ω_τ in the infrared range which dominates in the dispersion relation for the dielectric function $\varepsilon(i\zeta)$. It was noted that one can find the upper limit on the Casimir force that realized for perfect single-crystal materials for which electrical and optical properties are well defined. The surface roughness and linear in temperature corrections were taken into consideration. It was shown that the upper limit on the Casimir force does not contradict to the result of the torsion pendulum experiment [9]. The main conclusion of the paper is that the upper limit is smaller than the observed force in the AFM experiments and the difference far exceeds experimental errors and theoretical uncertainties for small separations between bodies. The simplest modification of the experiment is proposed allowing to reveal origin of the discrepancy.

[1] H.B.G. Casimir, Koninkl. Ned. Akad. Wetenschap. Proc. **51**, 793 (1948).
[2] V.M. Mostepanenko and N.N. Trunov, *The Casimir effect and its applications* (Clarendon Press, Oxford, 1997).
[3] E.M. Lifshitz, Sov. Phys. JETP **2**, 73 (1956).
[4] E.M. Lifshitz and L.P. Pitaevskii, *Statistical Physics, Part 2*, (Pergamon Press, Oxford, 1980).
[5] V.A. Kuz'min, I.I. Tkachev, and M.E. Shaposhnikov, JETP Letters (USA) **36**, 59 (1982).
[6] V.M. Mostepanenko and I.Yu. Sokolov, Phys. Lett. **A 125** , 405 (1987).
[7] J.C. Long, H.W. Chan, and J.C. Price, Nucl. Phys. **B 539**, 23, (1999).
[8] E. Fischbach and C. Talmadge, *The Search for Non-Newtonian Gravity* (AIP Press/Springer-Verlag, New York, 1999).
[9] S.K. Lamoreaux, Phys. Rev. Lett. **78**, 5 (1997); **81**, 5475(E) (1998).
[10] U. Mohideen and A. Roy, Phys. Rev. Lett. **81** , 4549 (1998); e-print physics/9805032.
[11] A. Roy and U. Mohideen, Phys. Rev. Lett. **82** , 4380 (1999).
[12] A. Roy, C. -Y. Lin, and U. Mohideen, Phys. Rev. **D 60**, 111101 (1999); e-print quant-ph/9906062.
[13] J.Blocki, J. Randrup, W.J. Swiatecki, and C.F. Tsang, Ann. Phys. (N.Y.) **105**,427 (1977).
[14] I. E. Dzyaloshinskii, E. M. Lifshitz, L. P. Pitaevskii, Sov. Phys. Uspekhi **4** (1961) 153.
[15] C. M. Hargreaves, Proc. Kon. Nederl. Acad. Wet. **B68** (1965) 231; J. Schwinger, L.L. DeRaad, Jr., and K.A. Milton, Ann. Phys. (N.Y.) **115**, 1 (1978).

[16] V.M. Mostepanenko and N.N. Trunov, Sov. J. Nucl. Phys. (USA) **42**, 812 (1985); V. B. Bezerra, G. L. Klimchitskaya, C. Romero, Mod. Phys. Lett. **A 12** (1997) 2623.
[17] J. Mehra, Physica **37**, 145 (1967); L.S. Brown and G.J. Maclay, Phys. Rev. **184**, 1272 (1969); J. Schwinger, L.L. DeRaad, Jr., and K.A. Milton, Ann. Phys. (N.Y.) **115**, 1 (1978).
[18] M. Bordag, G.L. Klimchitskaya, and V.M. Mostepanenko, Int. J. Mod. Phys **A 10**, 2661 (1995).
[19] G. L. Klimchitskaya, A. Roy, U. Mohideen, and V. M. Mostepanenko, Phys. Rev. **A 60**, 3487 (1999); e-print quant-ph/9906033.
[20] S.K. Lamoreaux, Phys. Rev. **A59** R3149 (1999).
[21] A. Lambrecht and S. Reynaud, Europ. Phys. J. D **8** 309 (2000); e-print quant-ph/9907105.
[22] A. Lambrecht and S. Reynaud, Phys. Rev. Lett., to appear; e-print quant-ph/9912085.
[23] V.B. Svetovoy and M.V. Lokhanin, e-print quant-ph/0001010.
[24] V.B. Bezerra, G.L. Klimchitskaya, V.M. Mostepanenko, e-print quant-ph/9912090.
[25] V.B. Svetovoy and M.V. Lokhanin, e-print quant-ph/0004004.
[26] S.K. Lamoreaux, e-print quant-ph/9907076.
[27] G. L. Klimchitskaya, U. Mohideen, and V. M. Mostepanenko, e-print quant-ph/0003091.
[28] P. Grosse, *Free electrons in solids*, (Springer-Verlag, Berlin,1979).
[29] B.N.J. Persson, J.E. Demuth, Phys. Rev. **B 31**, 1856 (1985).
[30] V.M. Zolotarev, V.N. Morozov, and E.V. Smirnov, *Optical constants of natural and technical mediums* (Chimiya, Leningrad,1984).
[31] *Handbook of Optical Constants of Solids,* E.D. Palik ed. (Academic Press, New York 1995).
[32] L. Lechevallier, G. Richon, J. Le Bas, and M. Bernole, Vacuum **41**, 1218 (1990).
[33] M. Bordag, B. Geyer, G.L. Klimchitskaya, and V.M. Mostepanenko, Phys. Rev. **D 58**, 075003 (1998).
[34] *Materials in mechanical engineering and automation. Handbook.* Edited by Yu.M. Pyatin, 2nd ed. (Mashinostroenie, Moskva, 1982).
[35] M. Bordag, B. Geyer, G. L. Klimchitskaya, and V. M. Mostepanenko, e-print hep-ph/0003011.
[36] D.S. Campbell and A.K. Morley, Rep. Prog. Phys. **34,** 283 (1971).
[37] J.R. Kirtley, S. Washburn, and M.J. Brady, Phys. Rev. Lett. **60**, 1546 (1988).

FIG. 1. This figure demonstrates validity of the Drude approximation for Al (triangles) and Au (circles) in the infrared range. The resistivity does not depend on frequency (left axis). Solid lines (right axis) show that $\varepsilon''(\omega)$ depends on ω according to (16) with the parameters given in Table I (entries 2).

FIG. 2. The residual force (21) as a function of sphere-plate separation a for TP experiment [9]. For the original value of sphere radius $R = 11.3\ cm$ the points of closest approach in (a) demonstrate presence of some unexplained force. With the corrected value $R = 12.5\ cm$ [26] the residual force is shown in (b). In this case there is no contradiction between theory and experiment.

FIG. 3. The Casimir force measured in the AFM experiment [10] (triangles). The solid line represents the upper limit on the force. The dotted line is taken from [19] where the Au/Pd layer was ignored and expansion (28) used for the finite conductivity correction. This expansion fails at small separations and Eq. (27) has to be used instead. The result is represented by the dashed line. The difference between the solid and dashed lines is due to Au/Pd layer.

FIG. 4. Comparison of the results of two AFM experiments. The data from [10] are marked by solid triangles and the data from [12] presented as the open squares. The obvious contradiction of two experiments made with the same technique is connected with unjustified assumption of the transparency of Au/Pd layer in [12]. The right data can be restored by simple shift all the open squares on 16 nm to larger separations (see explanations in the text) and after that the experiments will agree with each other.

FIG. 5. The data from [12] shifted on 16 nm (open squares) and the upper limit on the Casimir force (solid line). The dashed line represents the force for the case when the 8 nm thick Au/Pd top layer is changed by Al with the maximal plasma frequency $\omega_p = 2.4 \cdot 10^{16}\ s^{-1}$.

FIG. 6. The residual force defined as (21) for the two AFM experiments. The data from [10] and [12] are presented as solid triangles and open squares, respectively. The figure demonstrates presence of some unexplained force which decreases rapidly with separation increase. The residual force is reproduced for both of the experiments.

Al	$\omega_p \cdot 10^{-16}$	$\omega_\tau \cdot 10^{-13}$	ρ_0 $\mu\Omega \cdot cm$
1^*	1.54 ± 0.01	15.5 ± 0.6	7.39
2	2.235 ± 0.001	12.49 ± 0.01	2.83
3	2.43 ± 0.05	14.4 ± 0.7	2.76
4^*	1.63 ± 0.03	18.2 ± 0.7	7.74
Au	$\omega_p \cdot 10^{-16}$	$\omega_\tau \cdot 10^{-13}$	ρ_0 $\mu\Omega \cdot cm$
1	1.280 ± 0.001	3.29 ± 0.05	2.27
2	1.3720 ± 0.0006	4.060 ± 0.002	2.44
3	1.34 ± 0.02	7.08 ± 0.18	4.46
4	1.0513 ± 0.0007	6.24 ± 0.21	6.40

TABLE I. Parameters of the Drude dielectric function (16) for Al and Au found by fitting the data [30] of different measurements in the infrared range ($\lambda > 2$ μm). The statistical errors of fitting are indicated. The resistivity was calculated via ω_p and ω_τ according to (17). The stars in the first column mark the data for film samples.

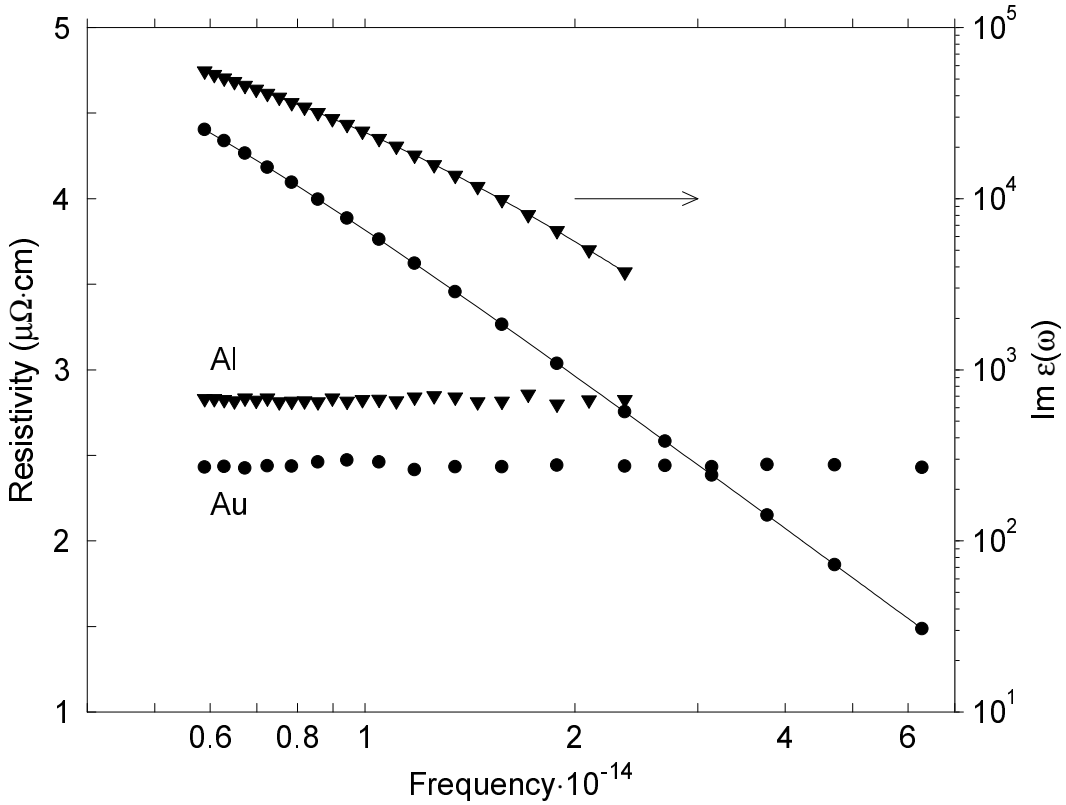
Resistivity (μΩ·cm)
Im ε(ω)
Frequency·10^-14
Al
Au
5
4
3
2
1
10^5
10^4
10^3
10^2
10^1
0.6
0.8
1
2
4
6

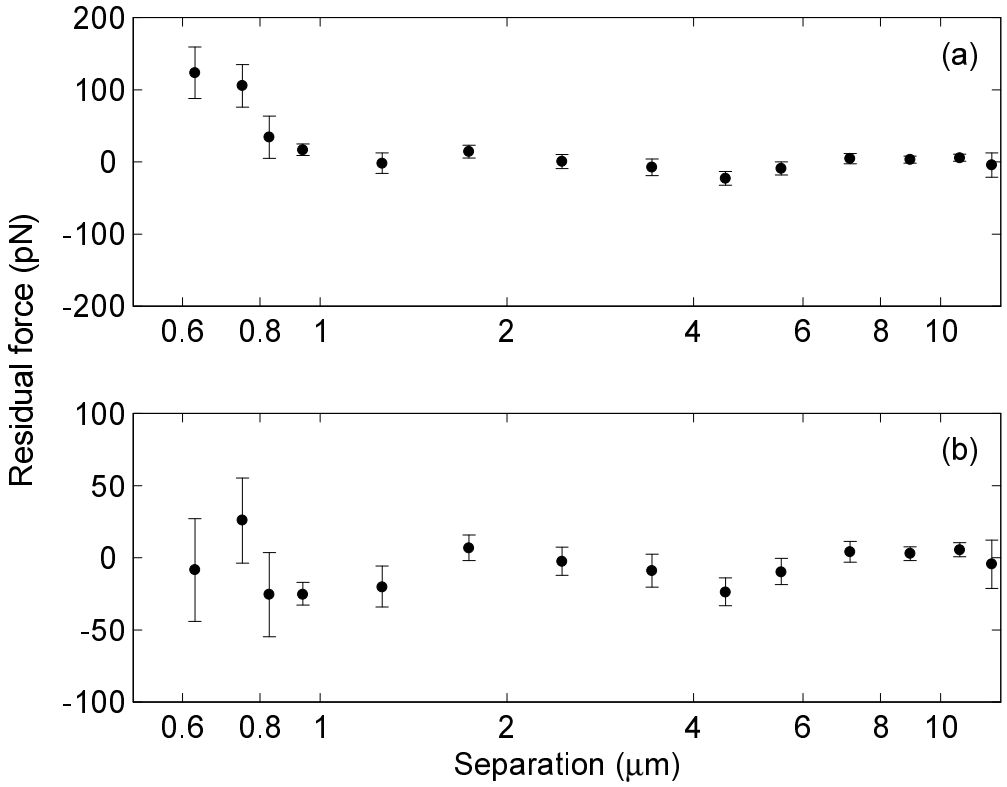
200
100
0
-100
-200
(a)
0.6
0.8
1
2
4
6
8
10
100
50
0
-50
-100
(b)
Residual force (pN)
Separation (μm)

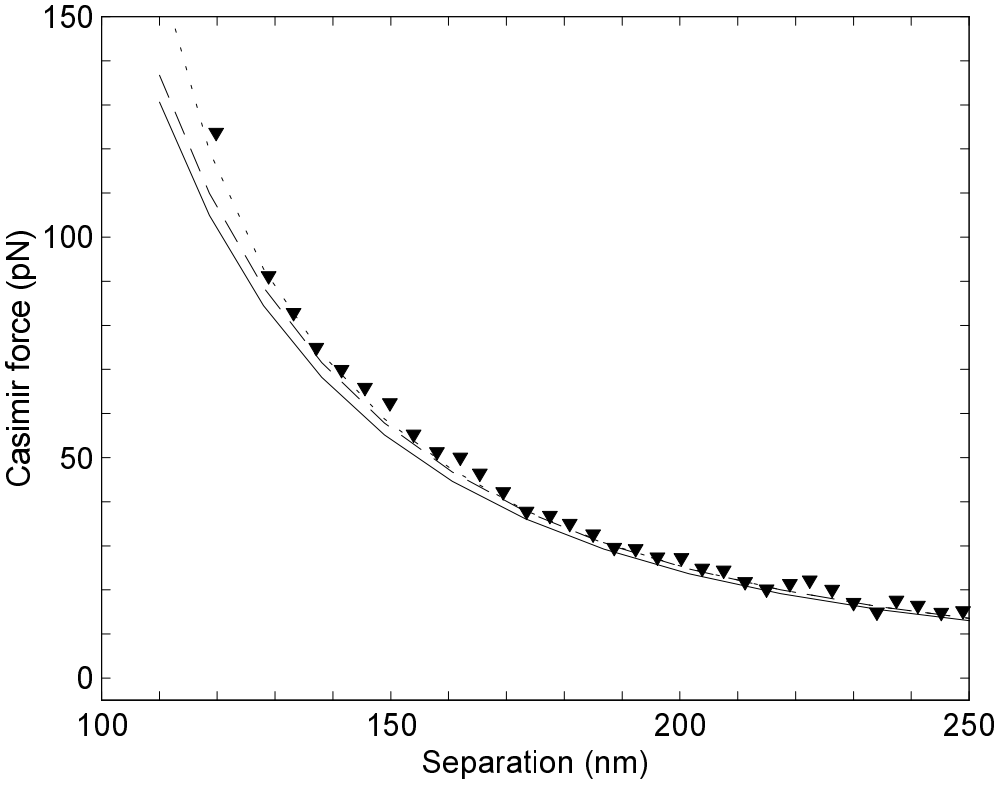
150
100
50
0
Casimir force (pN)
100
150
200
250
Separation (nm)

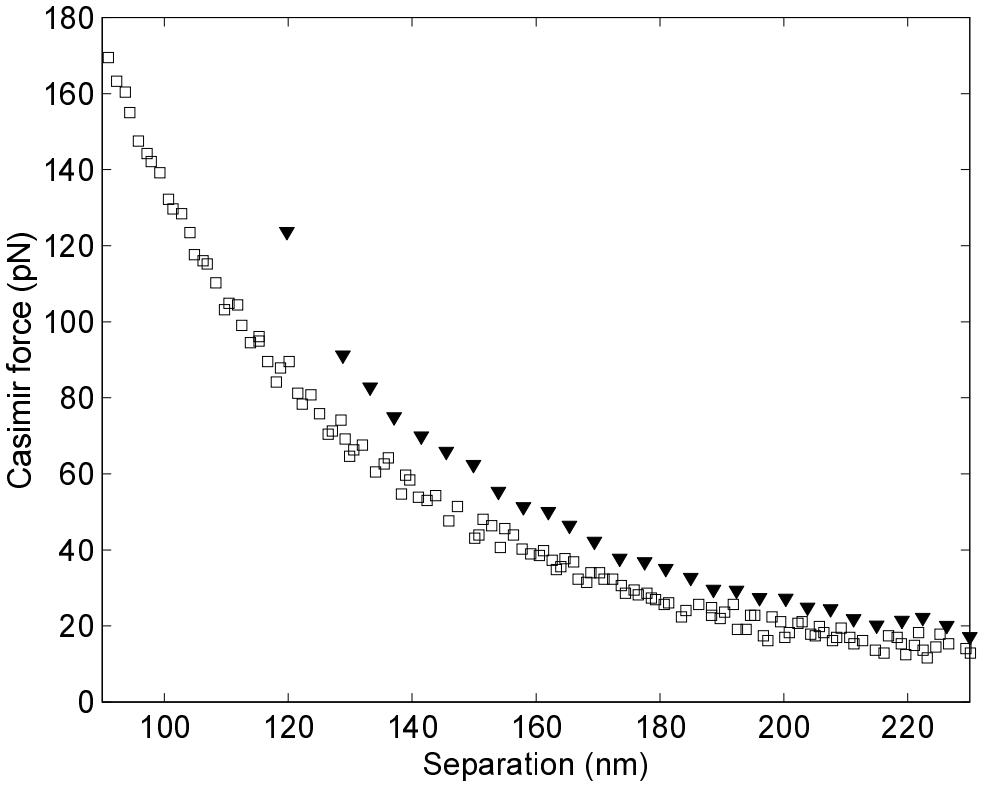
Casimir force (pN)
Separation (nm)
0
20
40
60
80
100
120
140
160
180
100
120
140
160
180
200
220

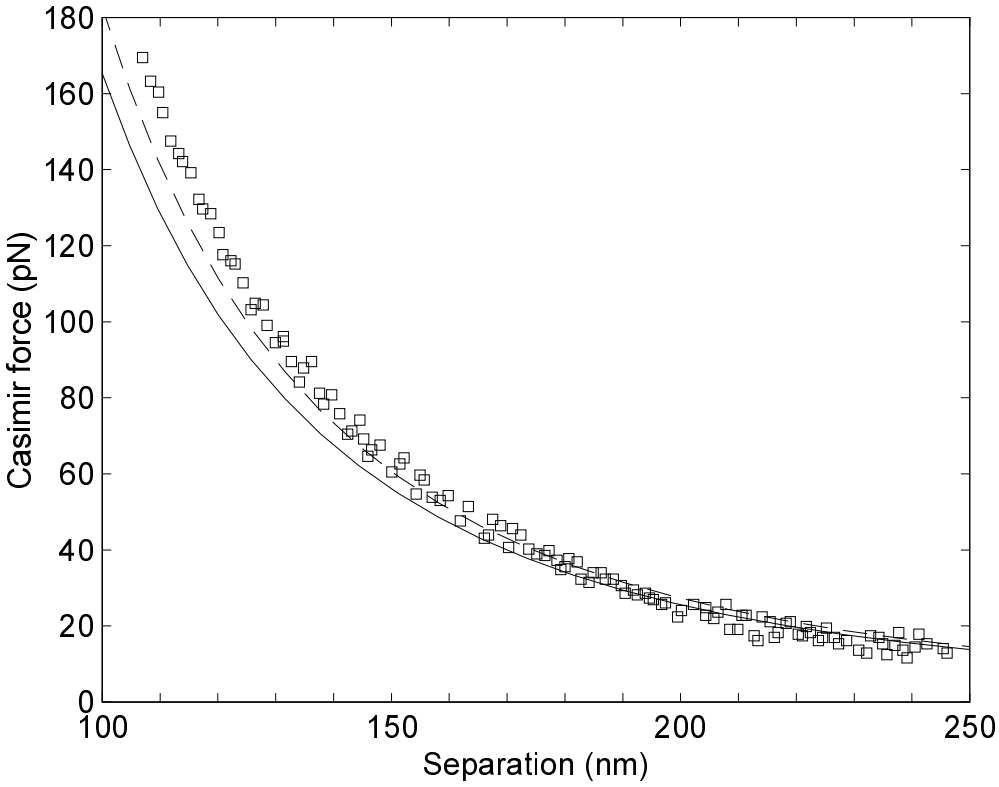
180
160
140
120
100
80
60
40
20
0
Casimir force (pN)
100
150
200
250
Separation (nm)

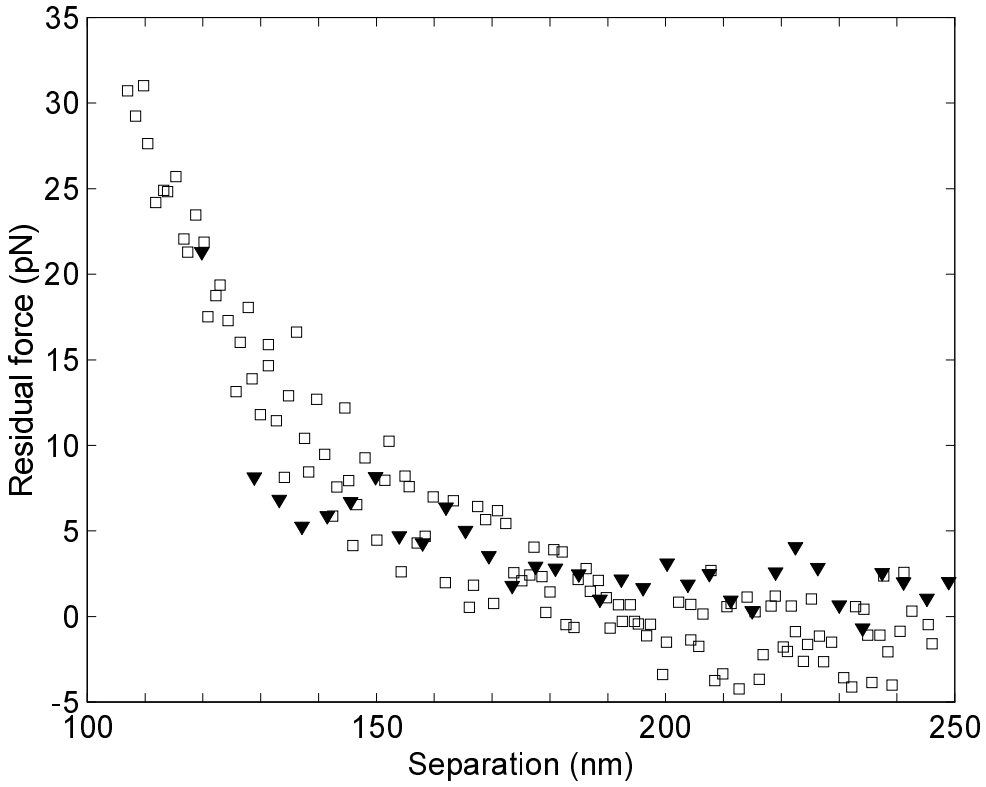
35
30
25
20
15
10
5
0
-5
Residual force (pN)
100
150
200
250
Separation (nm)